Supplementary Information:

Ion Specific Effects in Carboxylate Binding Sites

Mark J. Stevens*,† and Susan L. B. Rempe*,‡

†*Center for Integrated Nanotechnologies, Sandia National Laboratories, Albuquerque, NM, 87185*

‡*Center for Biological and Engineering Sciences, Sandia National Laboratories, Albuquerque, NM, 87185*

E-mail: msteve@sandia.gov; slrempe@sandia.gov

Atomic charges and induced ligand dipole moments

Atomic charges, q, were calculated using the atoms in molecules (AIM) method,[1] and ligand dipoles were calculated from the AIM partial charges. We caution that different methods yield different partial charges and that the dipole moment calculations are more sensitive since the ligand is charged, which makes the dipole moment depend on the geometry. To remove this geometry dependence in our comparison, we used the same geometry for the ligand in the dipole calculation. The cluster was oriented using the case of the n=1 ion-acetate complex as the template. One acetate molecule was chosen and oriented as the $n = 1$ complex. Specifically, the chosen acetate molecule is oriented with the carbonyl carbon at the origin and the carbon-carbon (C-C) bond vector of the acetate ligand pointing toward the ion on the x-axis and the oxygen-carbon-oxygen (OCO) atoms placed in the plane perpendicular to the y-axis. The rest of the atoms in the optimized structure are rotated by the transformation that rotates the first molecule into the given position. This geometry is used to calculate the dipole moments.

The dipole moments give insight on the structural preferences and indicate the amount of polarization as the number of ligands is varied. Those properties can guide force field development. Figure S1 shows the dipole magnitude (μ) as a function of the number of acetate ligands (n), calculated as described in the Methods and Validation section. For all ions, μ tends to decrease with n. In most cases, the dipole values level off at greater ligand numbers, making $n = 3$ and $n = 4$ values similar. The ligand changes to a monodentate orientation at $n = 3$ for most monovalent ions (except Cs^+), with one O atom closer to the ion than the other O atom. For the divalent ions, the orientation changes at $n = 4$. Thus, the dipole moment decreases monotonically in Figure S1 up to ligand reorientation for most ions. For each n, the Li^+ system has the largest μ of the singly charged ions, which decreases with increasing ion size for the monovalent ions. The dipole moments for the two divalent cases are larger than the monovalent ions, indicating a stronger ligand polarization with the divalent ions. Interestingly, the +2 charge of the divalent ions induces the same dipole

moments for each set of acetate ligands, masking the size difference between Zn^{2+} and Ca^{2+}.

The trends generally mirror those found earlier using DFT calculations on ion-water clusters,[2–4] but the μ values for acetates are larger, indicating more polarizable ligands. Because the acetate ligand is charged, there are also fundamental differences in dipole moment in comparison with neutral ligands such as water or formamide.[5] The dipole moment of the acetate ion depends on the origin chosen for the calculation. Thus, examining trends is valid, but comparing the magnitude of single cases is not as informative. For example, using the center of mass as the origin shifts the μ vs. n curves upward, but the trends remain the same. Also, the ion causes all the polarization in the case of a neutral ligand. For a charged ligand, there can be secondary ligand-ligand polarization effects. In addition, the increased number of atoms in an acetate ligand compared with water provides a larger region for charge delocalization.

The charge on the ion as a function of n is given in Figure S2. The plot shows the charge difference with respect to the ion valence and normalized by the valence, $(q - z)/z$. All the ions have a charge (q) lower than their valence (z). Cs^+ is an outlier compared with the smaller monovalent ions. The Cs^+ ion retains the most charge, with Li^+, Na^+ and K^+ losing slightly more charge and showing little difference within the group. Unsurprisingly, the divalent ions lose the most charge. As a consequence, the normalized charge difference $(q - z)/z$ is most negative for the divalent ions and increases to less negative values in the order of smallest to largest in the divalents and monovalents: $Zn^{2+} < Ca^{2+} < Li^+ \sim Na^+ \sim K^+ < Cs^+$ (Fig. S2). In contrast, the dipole moment depends only on q and is most positive for the divalent ions. Thus, the order is reversed in Figure S1 relative to Figure S2. Using the n=1 ion-acetate cluster as an example, the ligand dipole moments (μ) decrease in smallest to largest order among divalents and monovalents as (Fig. S1): $Zn^{2+} \sim Ca^{2+} > Li^+ \ldots Cs^+$.

Overall, these trends in ion and carboxylate electrostatic properties support the ligand field strength hypothesis. While cation charge shows little sensitivity to the number of

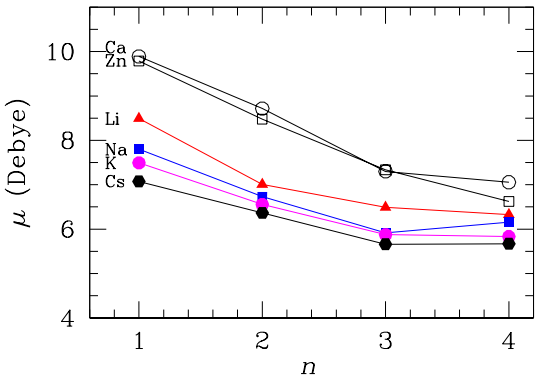

Figure S1: Average dipole moments of a single acetate ligand as a function of the number of ligands, n, in complex with each metal ion. The dipole moment of an isolated single acetate molecule provides a point of comparison, μ=5.44 D.

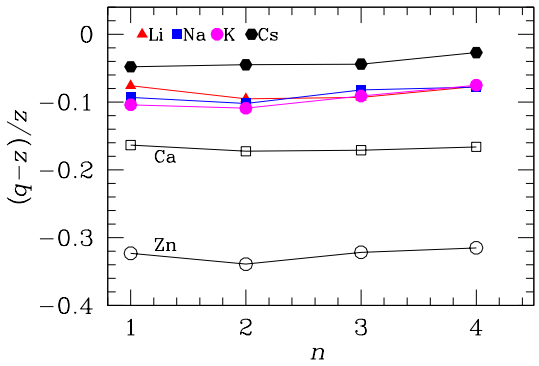

Figure S2: Cation charge (q) relative to formal charge (z=+1 for monovalents and +2 for divalents) as a function of the number of acetate ligands, n, in the ion-ligand complexes.

acetates, ligand dipole moment changes substantially with n. That sensitivity supports development of force fields that can capture changes in ligand dipoles, potentially by scaling fixed partial charges, as done recently for ionomers and carbonate solvents.[6,7]

$\Delta\Delta G$ Calculation

We represent the environment by a polarizable dielectric continuum model (PCM).[8] The PCM model includes contributions to the solvation free energy from electrostatic, packing, and dispersion terms. Default atomic radii were used to define cavities for the PCM model based on a set of overlapping spheres. The dielectric constant of the solvation environment

was set to mimic water at room temperature ($\epsilon = 78$). The ion-water complexes were reoptimized in the presence of the environment. Hydration free energies (ΔG_{aq}) were calculated at standard conditions of temperature (298 K) and pressure (1 atm) by adding the gas phase contribution (ΔG) to the contributions from the external environment (ion-water complexes and isolated waters) in the correct stoichiometric ratios,

$$\Delta G = G_p - \Sigma n_r G_r. \tag{S1}$$

The calculations assume a ligand density that corresponds to a pressure factor of 1 atm. In the final step, the ligand density was adjusted to account for the actual concentration of water ligands in liquid water, 1 g cm^{-3}, to match experimental conditions. The density correction corresponds to a pressure factor of 1354 atm, and thus adjusts the ion hydration free energy by $-k_B T \ln(1354/1)$, where k_B is the Boltzmann factor and T is the absolute temperature. Further details on application of quasi-chemical theory to ion hydration can be found in Refs.[9,10]

Data Tables

Tables S1 and S3 contain the free energies plotted in Fig. 1. The enthalpies for the monovalent ions are given in Table S2, and included in Table S3 for the divalent ions. The enthalpic terms follow the same trends as free energy, with the most favorable contributions for n=2 acetates around the monovalent ions, and n=3 acetates around the divalent ions. The enthalpic term also makes a large and favorable contribution to the free energy for all clusters, as expected for systems with strong electrostatic interactions. The unfavorable entropic term contributes a growing fraction to the overall free energy that becomes comparable in magnitude to enthalpy for n=4 acetate ligands, but still smaller. The entropic term shows little dependence on ion size. The geometries of the optimized structures are given in Tables S4-S9. Tables S10 and S11 contain the free energies differences plotted in Figs. 5 and 6. All

free energy, enthalpy, and structural results show ordering in terms of ion size, in support of the ligand field strength hypothesis. That trend is disrupted when ions transfer from aqueous solution to ion-carboxylate clusters (Tables S10 and S11).

Table S1: Free energies (ΔG in kcal/mol) for formation of ion-ligand complexes composed of one monovalent ion and n acetate ligands in a low dielectric environment ($\epsilon = 1$), as in Fig. 1.

n	Li	Na	K	Cs
1	-162.8	-138.8	-118.7	-99.0
2	-204.9	-179.2	-149.8	-132.2
3	-152.8	-129.9	-106.2	-93.0
4	-42.5	-28.3	-14.1	-12.2

Table S2: Enthalpies (ΔH in kcal/mol) for formation of ion-ligand complexes composed of one monovalent ion and n acetate ligands in a low dielectric environment ($\epsilon = 1$).

n	Li	Na	K	Cs
1	-170.8	-145.3	-127.6	-104.4
2	-219.4	-192.1	-168.4	-141.3
3	-175.7	-148.2	-129.5	-105.9
4	-73.7	-56.7	-45.4	-30.4

Table S3: Free energies (ΔG in kcal/mol) for formation of ion-ligand complexes composed of one divalent ion and n acetate ligands in a low dielectric environment ($\epsilon = 1$), as in Fig. 1.

n	Zn		Ca	
	ΔG	ΔH	ΔG	ΔH
1	-412.5	-421.8	-316.7	-321.2
2	-609.4	-628.2	-480.5	-492.2
3	-640.6	-681.6	-527.6	-545.8
4	-594.9	-638.2	-482.8	-505.9

Table S4: Bond lengths or pair distances (Å) and bond or triplet angles (deg) in optimized structures for Li^+ complexes with varying number of acetate ligands (n).

quantity	$n=1$	$n=2$	$n=3$	$n=4$
r(O- -Li)	1.852	2.027	1.903	2.102
r(C-O)	1.278	1.267	1.275	1.266
r(C-O)$_a$			1.255	
r(C-C)	1.513	1.532	1.544	1.547
$\angle$(C-O- -Li)	82.7	84.8	137.8	134.5
$\angle$(O- -Li- -O)	73.7	66.8	120.0	107.6
$\angle$(O- -Li- -O)				113.2
$\angle$(O-C-O)	120.8	123.4	126.5	127.0
$\angle$(C-C-O)	119.6	118.2	115.8	115.9
$\angle$(C-C-O)$_a$			117.7	117.3

[a] For oxygen (O) atoms far from the Li^+ ion.

Table S5: Bond lengths or pair separations (Å) and bond or triplet angles (deg) in optimized structures for Na^+ complexes with varying number of acetate ligands (n).

quantity	$n=1$	$n=2$	$n=3$	$n=4$
r(O- -Na)	2.193	2.345	2.228	2.431
r(C-O)	1.274	1.267	1.268	1.265
r(C-C)	1.521	1.536	1.551	1.550
$\angle$(C-O- -Na)	87.6	88.9	159.4	139.8
$\angle$(O- -Na- -O)	61.5	57.3	120.0	106.0
$\angle$(O- -Na- -O)$_a$				116.0
$\angle$(O-C-O)	123.4	124.9	127.6	127.0
$\angle$(C-C-O)	118.3	117.5	115.1	115.8
$\angle$(C-C-O)$_a$			117.3	116.7

[a] This is for the O atoms far from Na^+ in the $n=3$ case.

Table S6: Bond lengths or pair separations (Å) and bond or triplet angles (deg) in optimized structures for K^+ complexes with varying number of acetate ligands (n).

quantity	$n=1$	$n=2$	$n=3$	$n=4$
r(O- -K)	2.505	2.700	2.592	2.850
r(C-O)	1.265	1.259	1.261	1.255
r(C-C)	1.522	1.538	1.552	1.554
∠(C-O- -K)	91.4	92.4	173.1	150.5
∠(O- -K- -O)	53.0	49.1	119.9	115.4/106.5
∠(O-C-O)	124.1	126.1	128.2	128.4
∠(C-C-O)	118.5	117.6	114.7	115.0
∠(C-C-O)	117.4	116.4	117.1_a	116.7_b

[a] This is for the O atoms far from K^+ in the $n=3$ case.

[b] The O positions for $n=4$ are not completely symmetric.

Table S7: Bond lengths or pair separations (Å) and bond or triplet angles (deg) in optimized structures for Cs^+ complexes with varying number of ligands (n).

quantity	$n=1$	$n=2$	$n=3$	$n=4$
r(O- -Cs)	2.970	3.162	3.414	3.370
r(C-O)	1.270	1.266	1.262	1.263
r(C-C)	1.533	1.543	1.555	1.556
∠(C-O- -Cs)	95.0	95.80	96.8	158.2
$\angle$(O- -Cs- -O)$_b$	44.65	41.90	38.7	110.2
$\angle$(O- -Cs- -O)$_a$				107.3
∠(O-C-O)	125.4	126.5	127.7	128.3
∠(C-C-O)	117.3	116.7	116.2	115.2
$\angle$(C-C-O)$_a$				116.5

[a] This is for the O far from Cs^+.

[b] For $n=4$, C-O- -Cs are only for O atoms closest to Cs^+.

Table S8: Bond lengths or pair separations (Å) and bond or triplet angles (deg) in optimized structures for Zn^{2+} complexes with varying number of acetate ligands (n).

quantity	$n=1$	$n=2$	$n=3$	$n=4$
r(O- -Zn)	1.965	2.036	2.178	1.994
r(C-O)	1.290	1.278	1.268	1.295
r(C-O)$_a$				1.243
r(C-C)	1.496	1.502	1.520	1.533
∠(C-O- -Zn)	86.9	88.1	88.8	128.9
∠(O- -Zn- -O)	68.4	65.3	61.1	110.2
∠(O-C-O)	117.8	118.6	121.5	124.0
∠(C-C-O)	121.1	120.7	119.2	116.6
$\angle$(C-C-O)$_a$				119.4

[a] This is for O atoms far from Zn^{2+}.

Table S9: Bond lengths or pair separations (Å) and bond or triplet angles (deg) in optimized structures for Ca^{2+} complexes with varying number of ligands (n).

quantity	$n=1$	$n=2$	$n=3$	$n=4$
r(O- -Ca)	2.146	2.303	2.414	2.241
r(C-O)	1.283	1.274	1.263	1.280
r(C-O)$_a$				1.238
r(C-C)	1.487	1.508	1.523	1.541
$\angle$(C-O- -Ca)	90.2	90.7	91.1	165.6
$\angle$(O- -Ca- -O)	61.7	57.6	54.7	109.8
$\angle$(O-C-O)	118.0	120.1	123.3	126.7
$\angle$(C-C-O)	121.0	118.5	118.5	114.4
$\angle$(C-C-O)$_a$				118.9

[a] This is for O atoms far from Ca^{2+}.

Table S10: The change in free energy ($\Delta\Delta G$ in kcal/mol) for ion transfer from aqueous solution to a binding site composed of one monovalent ion and n acetate ligands in a low dielectric environment ($\epsilon = 1$), as in Figs. 5 and 6.

n	Li	Na	K	Cs
1	-45.5	-46.4	-44.4	-33.3
2	-87.6	-88.2	-75.5	-62.9
3	-35.5	-38.9	-31.9	-23.2
4	74.8	62.7	60.2	59.7

Table S11: The change in free energy ($\Delta\Delta G$ in kcal/mol) for ion transfer from aqueous solution to a binding site composed of one divalent ion and n acetate ligands in a low dielectric environment ($\epsilon = 1$), as in Figs. 5 and 6.

n	Zn	Ca
1	58.5	46.8
2	-134.8	-117.0
3	-169.6	-164.1
4	-123.9	-119.2

References

(1) Slee, T.; Larouche, A.; Bader, R. Properties of Atoms in Molecules: Dipole Moments and Substituent Effects in Ehtyl and Carbonyl Compounds. *J. Phys. Chem.* **1988**, *92*, 6219–6227.

(2) Krekeler, C.; Site, L. D. Solvation of Positive Ions in Water: The Dominant Role of Water–Water Interaction. *J. Phys.: Condens. Matter* **2007**, *19*, 192101.

(3) Varma, S.; Rempe, S. B. Multibody Effects in Ion Binding and Selectivity. *Biophys. J.* **2010**, *99*, 3394–3401.

(4) Soniat, M.; Rogers, D. M.; Rempe, S. B. Dispersion- and Exchange-Corrected Density Functional Theory for Sodium Ion Hydration. *J. Chem. Theory Comput.* **2015**, *11*, 2958–2967.

(5) Rossi, M.; Tkatchenko, A.; Rempe, S. B.; Varma, S. Role of Methyl-Induced Polarization in Ion Binding. *Proc. Natl. Acad. Sci. U.S.A.* **2013**, *110*, 12978–12983.

(6) Beichel, W.; Trapp, N.; Hauf, C.; Kohler, O.; Eickerling, G.; Scherer, W.; Krossing, I. Charge-Scaling Effect in Ionic Liquids from the Charge-Density Analysis of N,N'-Dimethylimidazolium Methyl-Sulfate. *Angew. Chem. Int. Ed.* **2014**, *53*, 3143–3146.

(7) Chaudhari, M. I.; Nair, J. R.; Pratt, L. R.; Soto, F. A.; Balbuena, P. B.; Rempe, S. B. Scaling Atomic Partial Charges of Carbonate Solvents for Lithium Ion Solvation and Diffusion. *J. Chem. Theory Comput.* **2016**, *DOI: 10.1021/acs.jctc.6b00824*.

(8) Tomasi, J.; Mennucci, B.; Cammi, R. Quantum Mechanical Continuum Solvation Models. *Chem. Rev.* **2005**, *105*, 2999–3093.

(9) Rogers, D. M.; Jiao, D.; Pratt, L. R.; Rempe, S. B. Structural Models and Molecular

Thermodynamics of Hydration of Ions and Small Molecules. *Ann. Rep. Comput. Chem.* **2012**, *8*, 71–128.

(10) Chaudhari, M. I.; Soniat, M.; Rempe, S. B. Octa-Coordination and the Aqueous Ba^{2+} Ion. *J. Phys. Chem. B* **2015**, *119*, 8746–8753.